Observation of the suppressed $\Lambda_b^0 \to DpK^-$ decay with $D \to K^+\pi^-$ and measurement of its CP asymmetry

R. Aaij *et al.*[*]
(LHCb Collaboration)

(Received 17 September 2021; accepted 12 October 2021; published 27 December 2021)

A study of Λ_b^0 baryon decays to the DpK^- final state is presented based on a proton-proton collision data sample corresponding to an integrated luminosity of 9 fb^{-1} collected with the LHCb detector. Two Λ_b^0 decays are considered, $\Lambda_b^0 \to DpK^-$ with $D \to K^-\pi^+$ and $D \to K^+\pi^-$, where D represents a superposition of D^0 and $\bar{D}^0$ states. The latter process is expected to be suppressed relative to the former, and is observed for the first time. The ratio of branching fractions of the two decays is measured, and the CP asymmetry of the suppressed mode, which is sensitive to the Cabibbo-Kobayashi-Maskawa angle γ, is also reported.

DOI: 10.1103/PhysRevD.104.112008

I. INTRODUCTION

Few studies of beauty-baryon decays to final states involving a single open-charm meson exist, but they are nonetheless promising for measurements of CP violation [1–3]. A measurement of a set of branching fraction ratios of Λ_b^0 and Ξ_b decays to final states including a D meson yielded the first observation of the singly Cabibbo-suppressed $\Lambda_b^0 \to [K^-\pi^+]_D pK^-$ decay [4], where D represents a D^0 or $\bar{D}^0$ meson.[1] This was followed by a study of the resonant structure of $\Lambda_b^0 \to D^0 p\pi^-$ decays [5]. This paper reports the results of a study of $\Lambda_b^0 \to DpK^-$ decays with the objectives of observing for the first time the $\Lambda_b^0 \to DpK^-$ decay with $D \to K^+\pi^-$, denoted as $\Lambda_b^0 \to [K^+\pi^-]_D pK^-$ and measuring its CP asymmetry. This decay is expected to be suppressed relative to the $\Lambda_b^0 \to [K^-\pi^+]_D pK^-$ decay. An estimate of the ratio of branching fractions between the favoured and suppressed modes is obtained by considering the relevant Cabibbo-Kobayashi-Maskawa (CKM) matrix elements [6]

$$R \approx \left|\frac{V_{cb}V_{us}^*}{V_{ub}V_{cs}^*}\right|^2 = 6.0. \tag{1}$$

The $\Lambda_b^0 \to [K^-\pi^+]_D pK^-$ ($\Lambda_b^0 \to [K^+\pi^-]_D pK^-$) decay with same (opposite) sign kaons are referred to as the favored (suppressed) decay throughout this paper. The suppressed decay is of particular interest since its decay amplitude receives contributions from $b \to c$ and $b \to u$ amplitudes of similar magnitude, given the CKM suppression between the two D decays. The interference between these two amplitudes, which depends upon the CKM angle γ, is expected to be large [7,8], but the different strong phases associated with the various configurations of polarization states for the Λ_b^0, proton, and intermediate resonances complicate determination of γ.

The analysis is based on proton-proton (pp) collision data collected with the LHCb detector at $\sqrt{s} = 7$, 8, and 13 TeV, corresponding to a total integrated luminosity of 9 fb^{-1}. The suppressed $\Lambda_b^0 \to [K^+\pi^-]_D pK^-$ decay is observed for the first time. In addition the ratio of branching fractions of the favored and suppressed decays, R, and the CP asymmetry in the suppressed mode, A, which is expected to be sensitive to the CKM angle γ, are measured where

$$R = \frac{\mathcal{B}(\Lambda_b^0 \to [K^-\pi^+]_D pK^-)}{\mathcal{B}(\Lambda_b^0 \to [K^+\pi^-]_D pK^-)},$$

including both flavors, and

$$A = \frac{\mathcal{B}(\Lambda_b^0 \to [K^+\pi^-]_D pK^-) - \mathcal{B}(\bar{\Lambda}_b^0 \to [K^-\pi^+]_D \bar{p}K^+)}{\mathcal{B}(\Lambda_b^0 \to [K^+\pi^-]_D pK^-) + \mathcal{B}(\bar{\Lambda}_b^0 \to [K^-\pi^+]_D \bar{p}K^+)}. \tag{2}$$

Sensitivity to CP violation requires interference between amplitudes involving intermediate D^0 and $\bar{D}^0$ mesons.

[*]Full author list given at the end of the article.

[1]Charge conjugation is implied throughout this document except in reference to CP asymmetries or comparisons of Λ_b^0 and $\bar{\Lambda}_b^0$ samples.

This interference is anticipated to be amplified in regions of the phase space involving $\Lambda_b^0 \to DX$ contributions, where X labels excited Λ states. Therefore, the ratio of branching fractions and the CP asymmetry in the suppressed mode are measured separately in the full phase space and in a restricted phase-space region which involves $\Lambda_b^0 \to DX$ decays, where an enhanced sensitivity to γ is expected.

II. DETECTOR AND SIMULATION

The LHCb detector [9,10] is a single-arm forward spectrometer covering the pseudorapidity range $2 < \eta < 5$, designed for the study of particles containing b or c quarks. The detector includes a high-precision tracking system consisting of a silicon-strip vertex detector surrounding the pp interaction region [11], a large-area silicon-strip detector located upstream of a dipole magnet with a bending power of about 4 Tm, and three stations of silicon-strip detectors and straw drift tubes [12,13] placed downstream of the magnet. The tracking system provides a measurement of the momentum, p, of charged particles with a relative uncertainty that varies from 0.5% at low momentum to 1.0% at 200 GeV/c. The minimum distance of a track to a primary pp collision vertex (PV), the impact parameter (IP), is measured with a resolution of $(15 + 29/p_{\mathrm{T}})\mu$m, where p_{T} is the component of the momentum transverse to the beam, in GeV/c. Different types of charged hadrons are distinguished using information from two ring-imaging Cherenkov detectors [14]. Hadrons are identified by a calorimeter system consisting of scintillating-pad and preshower detectors, an electromagnetic and a hadronic calorimeter. The online event selection is performed by a trigger [15], which consists of a hardware stage, based on information from the calorimeter, followed by a software stage, which applies a full event reconstruction.

Simulation is required to model the effects of the detector acceptance and the imposed selection requirements. In the simulation, pp collisions are generated using Pythia [16] with a specific LHCb configuration [17]. Decays of unstable particles are described by EvtGen [18], in which final-state radiation is generated using Photos [19]. The interaction of the generated particles with the detector, and its response, are implemented using the Geant4 toolkit [20] as described in Ref. [21].

The particle identification (PID) response in the simulated samples is corrected using control samples of $\Lambda_c^+ \to pK^-\pi^+$ decays in LHCb data, taking into account its correlation with the kinematic properties of each track and with the event multiplicity. To parametrize the PID response, an unbinned method is employed, where the probability density functions (PDFs) are modeled using kernel density estimation [22].

III. RECONSTRUCTION AND SELECTION OF CANDIDATES

Neutral D meson candidates are reconstructed by combining kaon and pion candidates having opposite charge. To form Λ_b^0 candidates, the neutral D meson candidates are combined with proton and kaon candidates having opposite charge. Each Λ_b^0 candidate is associated to the PV for which the value of χ^2_{IP} is minimized, where χ^2_{IP} is the difference between the vertex χ^2 of a given PV with and without the Λ_b^0 candidate included in the PV fit. The tracks forming the Λ_b^0 candidate are required to have good fit quality and to be well separated from any PV in the event. The invariant masses of the Λ_b^0 candidate, $M(DpK^-)$, and of the D candidate, $M(K\pi)$, are required to be in the intervals from 5200 to 7000 MeV/c^2 and 1850 to 1880 MeV/c^2, respectively. Candidates with $M(K\pi)$ in a wider mass range from 1765 to 1965 MeV/c^2 are retained to quantify the background contribution from charmless b -hadron decays. A kinematic fit is performed in which $M(K\pi)$ is constrained to the known D^0 mass [6] and the Λ_b^0 candidate's trajectory is required to point back to the associated PV [23]. To improve the resolution of the squared invariant masses $M^2(Dp)$, $M^2(DK^-)$ and $M^2(pK^-)$, the fit is repeated when calculating these variables, with the additional constraint that the invariant mass of the DpK^- combination is equal to the known Λ_b^0 mass [6] and is applied when calculating these variables. Inclusion of the mass constraint improves the resolution on the two-body masses by 50% or more, depending upon position in the three-body phase space.

Background from $\Lambda_b^0 \to \Lambda_c^+ h^-$ decays, with $\Lambda_c^+ \to ph^-h^+$ where h is a charged kaon or pion, is vetoed by requiring that the invariant mass of any ph^-h^+ combination differs from the known Λ_c^+ mass [6] by more than 20 MeV/c^2. To suppress the contribution of events from charmless $\Lambda_b^0 \to ph^-h^+h^-$ decays, the decay-time significance of the D meson candidates with respect to the Λ_b^0 vertex is required to be larger than 2.5. The decay-time significance of the D candidate is defined as the measured decay time divided by its uncertainty.

To suppress combinatorial background, a boosted decision tree (BDT) algorithm using adaptive boosting [24] is employed as implemented in the TMVA toolkit [25]. To train the BDT classifier, one for the full and another for the restricted phase space, a sample of simulated $\Lambda_b^0 \to [K^-\pi^+]_D pK^-$ decays is used as a proxy for signal and candidates in the Λ_b^0 mass sidebands with mass in the intervals from 5300 to 5400 MeV/c^2 and from 5900 to 6000 MeV/c^2 are used to represent combinatorial background. The variables that enter the BDT selection are the quality of the kinematic fit, the quality of the Λ_b^0 and D vertices and their decay-time significances, PID variables, and the p_{T} of the final-state particles. The optimization criterion used to determine the choice of BDT working

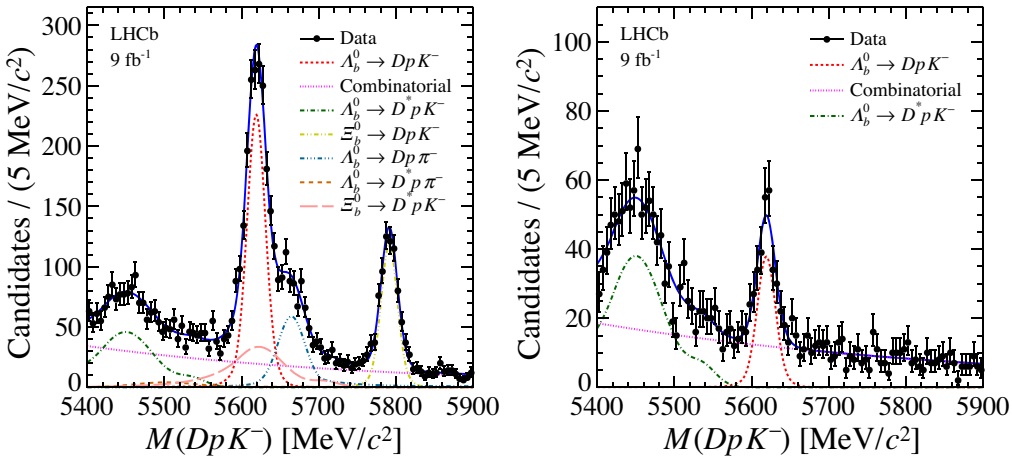

FIG. 1. Distributions of the invariant mass for selected (left) $\Lambda_b^0 \to [K^-\pi^+]_D pK^-$ and (right) $\Lambda_b^0 \to [K^+\pi^-]_D pK^-$ candidates in the full phase space (black points) corresponding to the favored and suppressed decays, respectively. The total fit model, as described in the text, is indicated by the solid blue line, and individual components are indicated.

point is the maximum expected statistical significance of the suppressed signal, $N_{\rm sig}/\sqrt{N_{\rm sig}+N_{\rm bkg}}$, where $N_{\rm sig}$ and $N_{\rm bkg}$ are the expected numbers of signal and background candidates in the mass interval from 5600 to 5640 MeV/c^2. The expected number of suppressed signal decays is determined by dividing the observed yield in the favored decay by the Cabibbo suppression factor defined in Eq. (1) using values for the CKM matrix elements taken from [26]. In 0.1% of events multiple Λ_b^0 candidates are reconstructed. All the candidates are retained.

IV. DETERMINATION OF SIGNAL YIELDS

The mass distributions for the DpK^- candidates in the favored and suppressed data samples in the full phase space are shown in Fig. 1. The number of signal candidates is obtained by an extended unbinned maximum-likelihood fit to the $M(DpK^-)$ mass distributions using the RooFit package [27]. The favored and suppressed samples are fitted simultaneously. The PDF used for the favored sample is made of two components to model $\Lambda_b^0 \to DpK^-$ and $\Xi_b^0 \to DpK^-$ signals, a background from misidentified $\Lambda_b^0 \to Dp\pi^-$ decays, and a partially reconstructed background from $\Lambda_b^0 \to D^*pK^-$ decays where $D^{*0} \to D^0\gamma$ or $D^{*0} \to D^0\pi^0$ and the γ or π^0 particle is not reconstructed. Additional components are required to describe the background due to partially reconstructed $\Lambda_b^0 \to D^*p\pi^-$ decays, with $D^{*0} \to D^0\gamma$ or $D^{*0} \to D^0\pi^0$ and having the pion from the Λ_b^0 decay misidentified as a kaon, partially reconstructed $\Xi_b^0 \to D^*pK^-$ decays, which peak in the signal region, and from combinatorial background. The PDF used to fit the suppressed sample is the same, except that it does not include contributions from the $\Xi_b^0 \to D^{(*)}pK^-$ and $\Lambda_b^0 \to D^{(*)}p\pi^-$ decays, which are expected to be negligible.

The parametrized shape of each component is taken from a fit to simulated decays after all selections are applied. The signal and partially reconstructed background are each modeled by the sum of two crystal ball (CB) functions [28], where the parameters governing the shape of the tails are fixed to their values in fits to simulated samples. The background from misidentified $\Lambda_b^0 \to Dp\pi^-$ decays is parametrized by the sum of a Gaussian and a CB function. In the restricted phase-space region, $M^2(pK^-) < 5\,{\rm GeV}^2/c^4$, the same functional forms are used, except that the partially reconstructed background is parametrized by the sum of a bifurcated Gaussian and a CB function. The combinatorial background is described by an exponential function. The slope of the combinatorial background is allowed to vary independently in the favored and suppressed samples. The widths of each peaking component are multiplied by a common free parameter in order to account for the difference between the invariant-mass resolution observed in data and simulation. The mass of the Λ_b^0 baryon is a free parameter, while the mass difference between Ξ_b^0 and Λ_b^0 baryons is fixed to its known value [6]. The yields of each component are allowed to vary independently in the favored and suppressed samples.

The projection of the fit to the invariant-mass distribution $M(DpK^-)$ in the favored and suppressed data samples in the full phase space is shown in Fig. 1. The Λ_b^0 yields are given in Table I. Figure 2 shows the invariant-mass

TABLE I. Signal Λ_b^0 yields obtained from fits to the invariant-mass distributions, $M(DpK^-)$, for the favored and suppressed decay samples in the two phase-space regions.

Phase-space region	$\Lambda_b^0 \to [K^-\pi^+]_D pK^-$	$\Lambda_b^0 \to [K^+\pi^-]_D pK^-$
Full	1437 ± 92	241 ± 22
Restricted	664 ± 36	84 ± 14

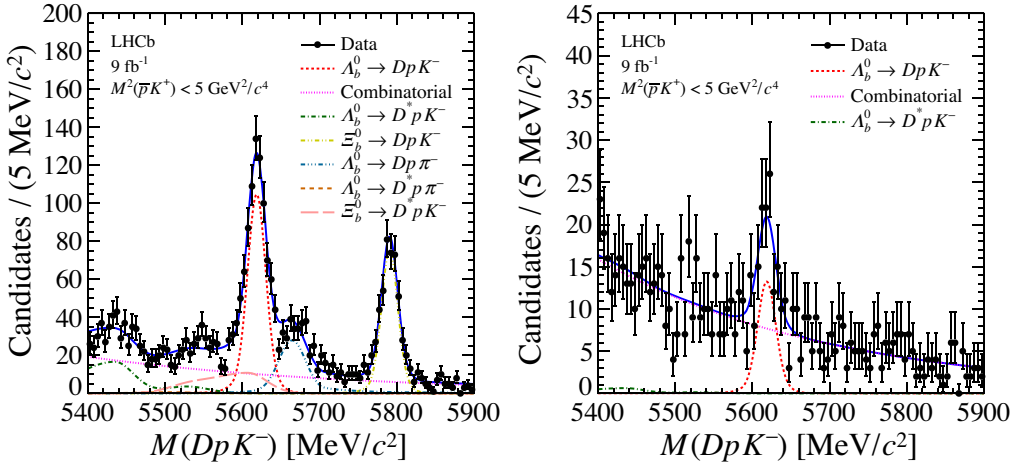

FIG. 2. Distributions of the invariant mass for (left) $\Lambda_b^0 \to [K^-\pi^+]_D pK^-$ and (right) $\Lambda_b^0 \to [K^+\pi^-]_D pK^-$ candidates, corresponding to the favored and suppressed decays, respectively, in the restricted phase-space region $M^2(pK^-) < 5\ \mathrm{GeV}^2/c^4$. The fit, as described in the text, is overlaid.

distribution $M(DpK^-)$ in the favored and suppressed data samples in the restricted phase-space region $M^2(pK^-) < 5\ \mathrm{GeV}^2/c^4$ with the fit projections overlaid. The signal yields obtained from this fit are given in Table I. The invariant-mass distributions $M(DpK^-)$ and $M(D\bar{p}K^+)$, overlaid with the fit projections, used to calculate the *CP* asymmetry of the suppressed decay in the full phase space and in the restricted phase-space region are shown in Figs. 3 and 4, respectively.

The resonant structure of the favored and suppressed decays can be illuminated by considering projections of the Λ_b^0 phase space. Figure 5 shows the $M^2(pK^-)$ versus $M^2(Dp)$ distributions of favored and suppressed candidates in the signal region $5600 < M(DpK^-) < 5640\ \mathrm{MeV}/c^2$. The signal purity in this region is 76% and 72% for the favored and suppressed modes, respectively. Despite the smaller combinatorial background, the signal purity for the favored decay is comparable to that for the suppressed decay due to the presence of the background from $\Xi_b^0 \to D^*pK^-$ and $\Lambda_b^0 \to Dp\pi^-$ decays in the signal region. Figures 6 and 7 show invariant-mass projections onto $M(pK^-)$, $M(Dp)$ and $M(DK^-)$ for selected candidates. The dominant resonant amplitudes in the favored mode could generate structures in the $M(Dp)$ and $M(pK^-)$ distributions, corresponding to states having *udc* and *uds* quark content, respectively. The $M(Dp)$ distribution shows an increased density of events in the low-$M(Dp)$ region with a contribution from $\Lambda_c(2860)^+ \to D^0 p$ decays. The distribution of $M(pK^-)$ contains a contribution from the $\Lambda(1520)$ baryon at low-$M(pK^-)$ and an enhancement at $2.5 \lesssim M(pK^-) \lesssim 3.5\ \mathrm{GeV}/c^2$, which is the reflection of the $\Lambda_c(2860)^+$ resonance seen in the $M(Dp)$ distribution.

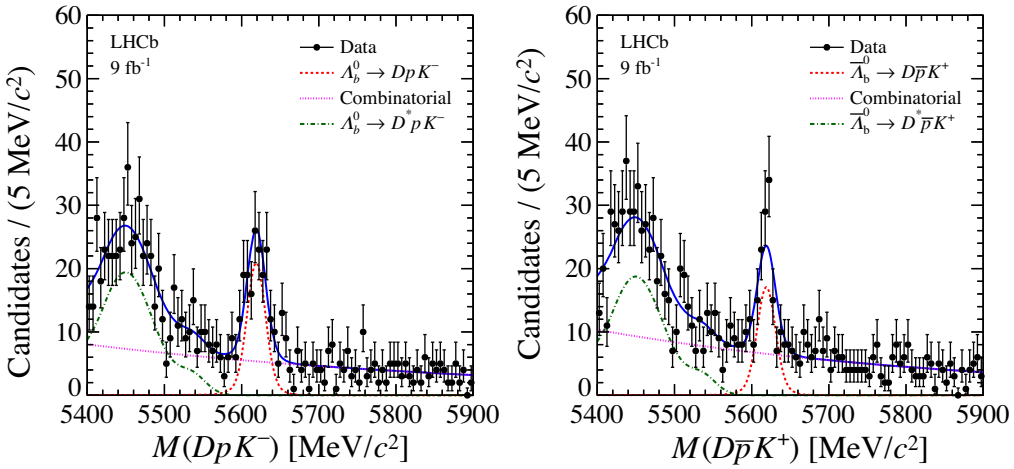

FIG. 3. Distributions of the invariant mass for (left) $\Lambda_b^0 \to [K^+\pi^-]_D pK^-$ and (right) $\bar{\Lambda}_b^0 \to [K^-\pi^+]_D \bar{p}K^+$ candidates in the full phase space (black points), corresponding to separation of the suppressed decay sample by Λ_b^0 flavour. The fit, as described in the text, is indicated by the solid blue line, and individual components are indicated.

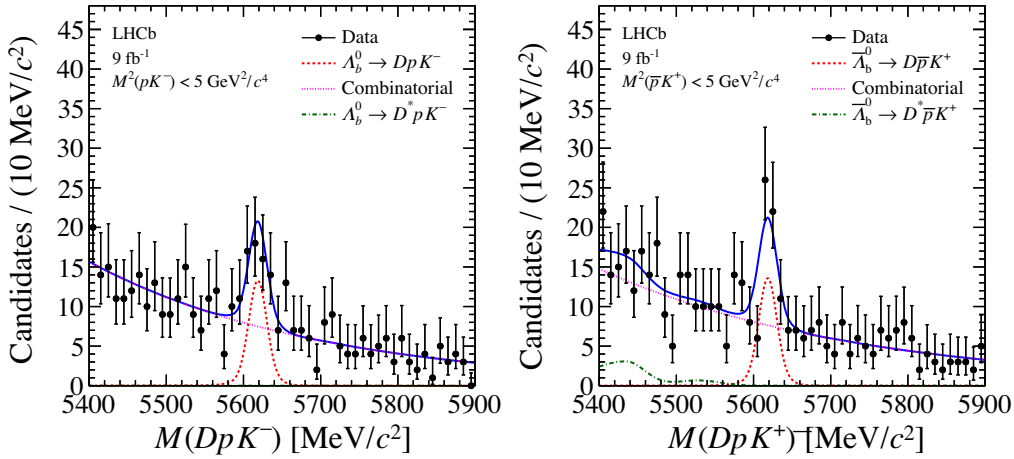

FIG. 4. Distributions of the invariant mass for (left) $\Lambda_b^0 \to [K^+\pi^-]_D pK^-$ and (right) $\bar{\Lambda}_b^0 \to [K^-\pi^+]_D \bar{p}K^+$ candidates in the restricted phase-space region (black points), where the separation is made according to the Λ_b^0 flavor. The fit, as described in the text, is indicated by the solid blue line, and individual components are indicated.

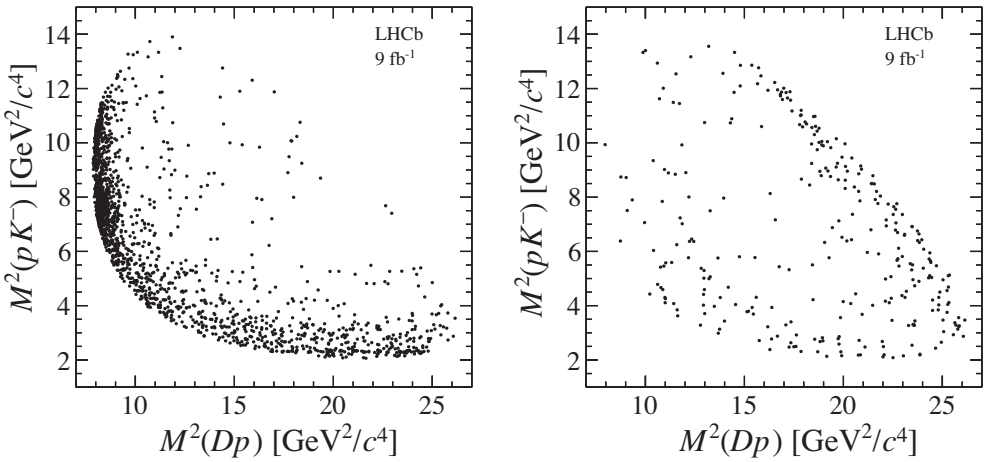

FIG. 5. Phase space of the (left) $\Lambda_b^0 \to [K^-\pi^+]_D pK^-$ and (right) $\Lambda_b^0 \to [K^+\pi^-]_D pK^-$ candidates having a mass between 5600 and 5640 MeV$/c^2$. No background subtraction is applied.

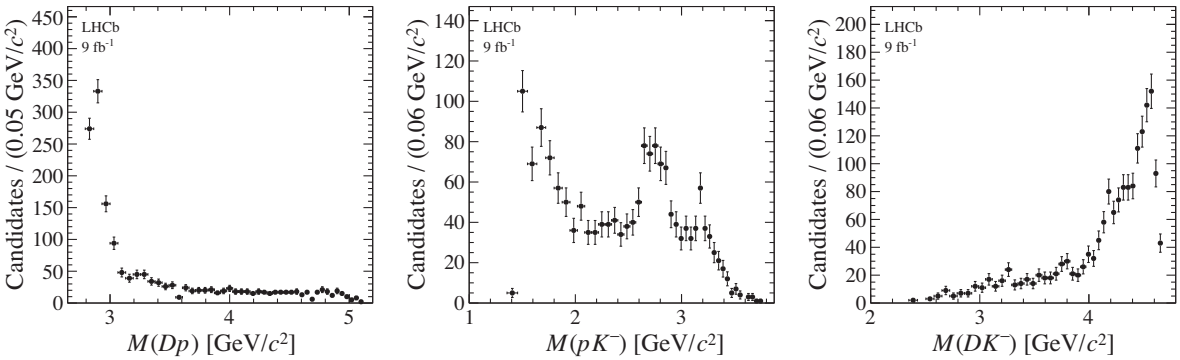

FIG. 6. Invariant-mass projections of the Λ_b^0 phase space in (left) $M(Dp)$, (middle) $M(pK^-)$, and (right) $M(DK^-)$ for the $\Lambda_b^0 \to [K^-\pi^+]_D pK^-$ candidates.

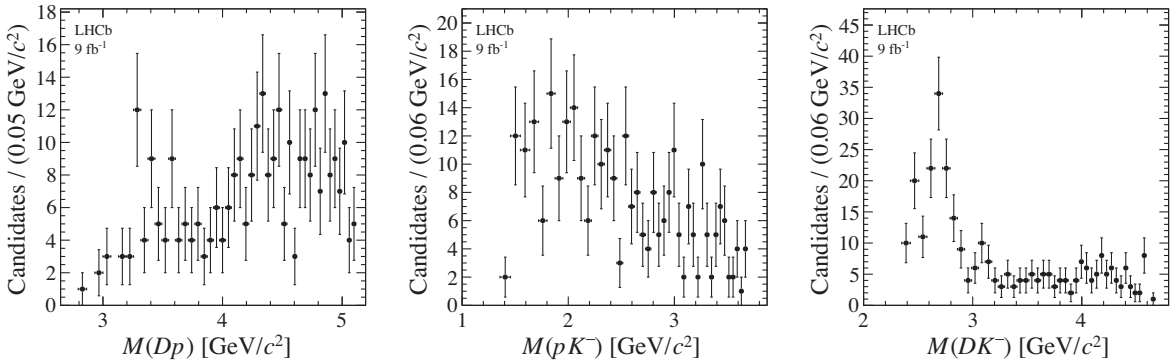

FIG. 7. Invariant-mass projections of the Λ_b^0 phase space in (left) $M(Dp)$, (middle) $M(pK^-)$, and (right) $M(DK^-)$ for the $\Lambda_b^0 \to [K^+\pi^-]_D pK^-$ candidates.

Different resonant structure is anticipated in the suppressed sample given the contributions from, and interference between, the $\Lambda_b^0 \to D^0 pK^-$ and $\Lambda_b^0 \to \bar{D}^0 pK^-$ amplitudes. The $M(DK^-)$ distribution in the suppressed sample shows an increased density of events in the low-mass region with a contribution from resonances decaying to DK^- such as the $D_{s1}^*(2700)^\pm$.

V. CALCULATION OF BRANCHING FRACTION RATIO AND *CP* ASYMMETRY

The ratio of branching fractions of the favored and suppressed decays and the *CP* asymmetry of the suppressed decay are calculated from the ratio of yields of the corresponding decays after applying efficiency correction factors as

$$R = \frac{\sum_i w^i_{\mathrm{FAV}}/\epsilon^i}{\sum_i w^i_{\mathrm{SUP}}/\epsilon^i}, \tag{3}$$

$$A = \frac{\sum_i w^i_{\mathrm{SUP},\Lambda_b^0}/\epsilon^i - \sum_i w^i_{\mathrm{SUP},\bar{\Lambda}_b^0}/\epsilon^i}{\sum_i w^i_{\mathrm{SUP},\Lambda_b^0}/\epsilon^i + \sum_i w^i_{\mathrm{SUP},\bar{\Lambda}_b^0}/\epsilon^i} \tag{4}$$

where the sum is over the selected candidates. Here w^i_{FAV} and w^i_{SUP} are the weights obtained using the *sPlot* technique [29] for background subtraction of the favored or suppressed samples, respectively, with $M(DpK^-)$ as the discriminating variable. The subscripts Λ_b^0 and $\bar{\Lambda}_b^0$ label the samples split by flavor and ϵ^i are the relative efficiencies. The efficiency corrections are determined as a function of the Λ_b^0 phase-space variables $M^2(Dp)$ and $M^2(pK^-)$ using the simulated $\Lambda_b^0 \to [K^-\pi^+]_D pK^-$ sample and parameterized by a kernel density estimation technique [22]. Across the phase space, the relative efficiencies vary from 0.7 to 1.2, as shown in Fig. 8.

The measured values of R and A in the full phase space with their statistical and systematic uncertainties are

$$R = 7.1 \pm 0.8(\mathrm{stat})^{+0.4}_{-0.3}(\mathrm{syst}),$$
$$A = 0.12 \pm 0.09(\mathrm{stat})^{+0.02}_{-0.03}(\mathrm{syst}),$$

and in the restricted phase-space region $M^2(pK^-) < 5\ \mathrm{GeV}^2/c^4$,

$$R = 8.6 \pm 1.5(\mathrm{stat})^{+0.4}_{-0.3}(\mathrm{syst}),$$
$$A = 0.01 \pm 0.16(\mathrm{stat})^{+0.03}_{-0.02}(\mathrm{syst}).$$

The data samples in the full and restricted phase-space region partially overlap and the statistical uncertainties on the ratios and asymmetries measured in these two regions are correlated. A positive correlation between the statistical uncertainties of $\rho = 0.33$ is estimated, given the number of events in the two samples and their overlap.

VI. SYSTEMATIC UNCERTAINTIES

The systematic uncertainties on the ratio of branching fractions of the favored and suppressed decays and the *CP*

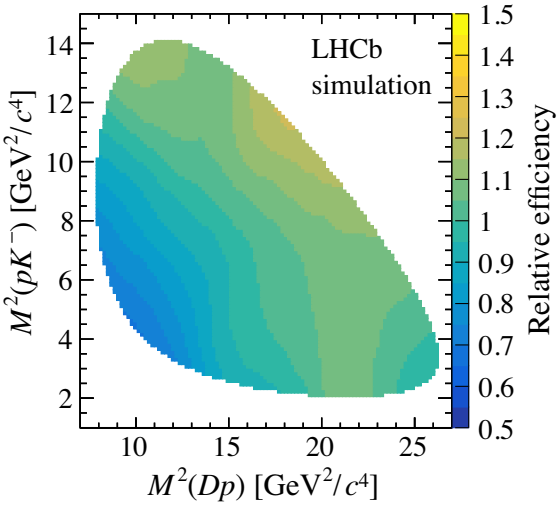

FIG. 8. Relative efficiency correction as a function of position within the Λ_b^0 phase space, obtained from simulated samples.

TABLE II. Absolute uncertainties on the ratio of branching fractions, R, and CP asymmetry, A, related to the sources of systematic uncertainty studied. The statistical and total systematic uncertainties are also shown.

	R	A
Systematic uncertainties		
Fit model	$^{+0.37}_{-0.15}$	$^{+0.000}_{-0.011}$
Efficiency corrections	$^{+0.21}_{-0.24}$	$^{+0.010}_{-0.008}$
PID efficiency	$^{+0.08}_{-0.16}$	$^{+0.001}_{-0.002}$
Hardware trigger efficiency	± 0.03	± 0.001
Charmless background	± 0.08	
Double misidentified background	± 0.005	
Single misidentified background	± 0.001	
Λ_b^0 production asymmetry		± 0.015
p detection asymmetry		± 0.015
π detection asymmetry		± 0.005
Total systematic uncertainty	$^{+0.43}_{-0.33}$	$^{+0.024}_{-0.026}$
Statistical uncertainty	± 0.79	± 0.088

asymmetry of the suppressed decay are listed in Table II. For each variation, the determination of R and A is performed, and the difference with respect to the nominal result is taken as systematic uncertainty. Where multiple variations are considered, the largest negative and positive deviations are taken. For the measurement of R and A, many systematic effects cancel in the ratios. The total systematic uncertainties are obtained by summing all the contributions in quadrature.

To assess systematic uncertainties due to the description of signal and background contributions in the invariant mass fit model, alternative parametrizations for the Λ_b^0 mass peak, partially reconstructed background components and combinatorial background are used. The corresponding systematic uncertainties amount to (1–5)%. The efficiency corrections are impacted by the limited size of the signal simulation sample. This is assessed by varying the parameters of the kernel density estimation. The corresponding systematic uncertainties are (1–3)%.

The PID response in data is obtained from calibration samples [30,31]. The associated systematic uncertainty includes the kernel width variation and the uncertainty due to finite sample size of the calibration samples. The resulting uncertainty is 2% for R, and less than 1% for A.

The hardware-level trigger decision is not perfectly simulated. The impact of this mismodeling is estimated by varying the efficiency map according to a correction obtained from data control samples. The resulting systematic uncertainty is at the level of 0.5%.

The background from charmless decays is estimated by interpolating from the D mass sidebands into the D mass region after all selection requirements are imposed and found to be 0.5% and 1% in the favored and suppressed samples, respectively. These values are taken as uncertainties and propagated to the measurement of R, resulting in an uncertainty of 1% on R, while the corresponding uncertainty on A is assumed to cancel.

Doubly misidentified background, where the kaon and pion in the favored mode are swapped, leads to a background that peaks at the Λ_b^0 mass in the suppressed sample. This contribution is estimated from simulation to be 0.5% in the suppressed sample, and this value is assigned as an uncertainty in R. Furthermore, the impact of $\Lambda_b^0 \to DpK^-$ decays with subsequent $D \to K^-K^+$ or $D \to \pi^-\pi^+$ decays, when one of the D decay products is misidentified, is found to be 0.1%.

The asymmetry in Λ_b^0 and $\bar{\Lambda}_b^0$ production is expected to influence the measurement of A. The average values were measured to be $(1.92 \pm 0.35)\%$ and $(1.09 \pm 0.29)\%$ at 7 and 8 TeV center-of-mass energies, respectively [32]. The production asymmetry is expected to decrease still further for a center-of-mass energy of 13 TeV [33,34]. A 1.5% systematic uncertainty is assigned. Furthermore, the detection asymmetry of the Λ_b^0 decay products is also expected to influence the measurement of A. The asymmetry in detecting protons versus antiprotons has been studied in detail [32] and does not exceed 1.5% for various values of proton momentum. The asymmetry of π^+ and π^- detection was studied in Ref. [35] and found to be less than 0.5%. These values are assigned as systematic uncertainties. Any influence of K^+ and K^- detection asymmetry is expected to cancel for the K^+ meson from the D meson and the K^- meson from the Λ_b^0 baryon.

Pseudoexperiments were used to verify that the fit used to determine the Λ_b^0 signal yields was unbiased, and no uncertainty from this source is included.

VII. CONCLUSION

A study of Λ_b^0 baryon decays to the $[K^\pm\pi^\mp]_D pK^-$ final state, where D indicates a superposition of D^0 and $\bar{D}^0$, is reported, using a data sample corresponding to an integrated luminosity of 9 fb^{-1} collected with the LHCb detector. The suppressed $\Lambda_b^0 \to [K^+\pi^-]_D pK^-$ decay is observed for the first time. The ratio of branching fractions for the $\Lambda_b^0 \to [K^-\pi^+]_D pK^-$ and $\Lambda_b^0 \to [K^+\pi^-]_D pK^-$ decays, and the CP asymmetry, are measured in the full phase space to be

$$R = 7.1 \pm 0.8(\text{stat})^{+0.4}_{-0.3}(\text{syst}),$$
$$A = 0.12 \pm 0.09(\text{stat})^{+0.02}_{-0.03}(\text{syst}).$$

In the phase-space region $M^2(pK^-) < 5\ \text{GeV}^2/c^4$ the ratio and CP asymmetry are measured to be

$$R = 8.6 \pm 1.5(\text{stat})^{+0.4}_{-0.3}(\text{syst}),$$
$$A = 0.01 \pm 0.16(\text{stat})^{+0.03}_{-0.02}(\text{syst}).$$

Within the uncertainties, the ratio of the favored and suppressed branching fractions is consistent with the

estimate based on the relevant CKM matrix elements. The measured asymmetry values are consistent with zero, both in the full phase space and in the region where enhanced sensitivity to the CKM angle γ is expected. While the present signal yields are too low to be used to extract γ, larger samples are expected to be collected by LHCb in the coming years, and the study of this mode will contribute to the overall determination of γ.

ACKNOWLEDGMENTS

We express our gratitude to our colleagues in the CERN accelerator departments for the excellent performance of the LHC. We thank the technical and administrative staff at the LHCb institutes. We acknowledge support from CERN and from the national agencies: CAPES, CNPq, FAPERJ and FINEP (Brazil); MOST and NSFC (China); CNRS/IN2P3 (France); BMBF, DFG and MPG (Germany); INFN (Italy); NWO (Netherlands); MNiSW and NCN (Poland); MEN/IFA (Romania); Ministry of Science and Higher Education (MSHE) (Russia); MICINN (Spain); SNSF and State Secretariat for Education and Research (SER) (Switzerland); NASU (Ukraine); STFC (United Kingdom); DOE NP and NSF (USA). We acknowledge the computing resources that are provided by CERN, IN2P3 (France), KIT and DESY (Germany), INFN (Italy), SURF (Netherlands), PIC (Spain), GridPP (United Kingdom), RRCKI and Yandex LLC (Russia), CSCS (Switzerland), IFIN-HH (Romania), CBPF (Brazil), PL-GRID (Poland) and NERSC (USA). We are indebted to the communities behind the multiple open-source software packages on which we depend. Individual groups or members have received support from ARC and ARDC (Australia); AvH Foundation (Germany); The European Particle physics Latin America NETwork (EPLANET), Marie Skłodowska-Curie Actions and ERC (European Union); Launch Of New Calls For Projects (A*MIDEX), ANR, Institute for Physics of the Universe (IPhU) and Labex P2IO, and Région Auvergne-Rhône-Alpes (France); Key Research Program of Frontier Sciences of CAS, CAS President's International Fellowship Initiative (PIFI), CAS CCEPP, Fundamental Research Funds for the Central Universities, and Sci. & Tech. Program of Guangzhou (China); RFBR, RSF and Yandex LLC (Russia); GVA, XuntaGal and GENCAT (Spain); the Leverhulme Trust, the Royal Society and UKRI (United Kingdom).

[1] I. Dunietz, *CP* violation with beautiful baryons, Z. Phys. C**56**, 129 (1992).
[2] Fayyazuddin, $\Lambda_b^0 \to \Lambda D^0(\bar{D}^0)$ decays and *CP* violation, Mod. Phys. Lett. A **14**, 63 (1999).
[3] A. K. Giri, R. Mohanta, and M. P. Khanna, Possibility of extracting the weak phase gamma from $\Lambda_b^0 \to \Lambda D^0$ decays, Phys. Rev. D **65**, 073029 (2002).
[4] R. Aaij *et al.* (LHCb Collaboration), Study of beauty baryon decays to $D^0 p h^-$ and $\Lambda_c^+ h^-$ final states, Phys. Rev. D **89**, 032001 (2014).
[5] R. Aaij *et al.* (LHCb Collaboration), Study of the $D^0 p$ amplitude in $\Lambda_b^0 \to D^0 p \pi^-$ decays, J. High Energy Phys. 05 (2017) 030.
[6] P. A. Zyla *et al.* (Particle Data Group Collaboration), Review of particle physics, Prog. Theor. Exp. Phys. **2020**, 083C01 (2020).
[7] D. Atwood, I. Dunietz, and A. Soni, Enhanced *CP* Violation with $B \to KD^0(\bar{D}^0)$ Modes and Extraction of the CKM Angle γ, Phys. Rev. Lett. **78**, 3257 (1997).
[8] D. Atwood, I. Dunietz, and A. Soni, Improved methods for observing *CP* violation in $B^\pm \to KD$ and measuring the CKM phase γ, Phys. Rev. D **63**, 036005 (2001).
[9] A. A. Alves Jr. *et al.* (LHCb Collaboration), The LHCb detector at the LHC, J. Instrum. **3**, S08005 (2008).
[10] R. Aaij *et al.* (LHCb Collaboration), LHCb detector performance, Int. J. Mod. Phys. A **30**, 1530022 (2015).
[11] R. Aaij *et al.*, Performance of the LHCb vertex locator, J. Instrum. **9**, P09007 (2014).
[12] R. Arink *et al.*, Performance of the LHCb outer tracker, J. Instrum. **9**, P01002 (2014).
[13] P. d'Argent *et al.*, Improved performance of the LHCb outer tracker in LHC run 2, J. Instrum. **12**, P11016 (2017).
[14] M. Adinolfi *et al.*, Performance of the LHCb RICH detector at the LHC, Eur. Phys. J. C **73**, 2431 (2013).
[15] R. Aaij *et al.*, The LHCb trigger and its performance in 2011, J. Instrum. **8**, P04022 (2013).
[16] T. Sjöstrand, S. Mrenna, and P. Skands, A brief introduction to PYTHIA 8.1, Comput. Phys. Commun. **178**, 852 (2008).T. Sjöstrand, S. Mrenna, and P. Skands, PYTHIA 6.4 physics and manual, J. High Energy Phys. 05 (2006) 026.
[17] I. Belyaev *et al.*, Handling of the generation of primary events in Gauss, the LHCb simulation framework, J. Phys. Conf. Ser. **331**, 032047 (2011).
[18] D. J. Lange, The EvtGen particle decay simulation package, Nucl. Instrum. Methods Phys. Res., Sect. A **462**, 152 (2001).
[19] N. Davidson, T. Przedzinski, and Z. Was, PHOTOS interface in C++: Technical and physics documentation, Comput. Phys. Commun. **199**, 86 (2016).
[20] J. Allison *et al.* (Geant4 Collaboration), Geant4 developments and applications, IEEE Trans. Nucl. Sci. **53**, 270 (2006); S. Agostinelli *et al.* (Geant4 Collaboration), Geant4: A simulation toolkit, Nucl. Instrum. Methods Phys. Res., Sect. A **506**, 250 (2003).
[21] M. Clemencic, G. Corti, S. Easo, C. R. Jones, S. Miglioranzi, M. Pappagallo, and P. Robbe, The LHCb simulation

application, Gauss: Design, evolution and experience, J. Phys. Conf. Ser. **331**, 032023 (2011).
[22] A. Poluektov, Kernel density estimation of a multidimensional efficiency profile, J. Instrum. **10**, P02011 (2015).
[23] W. D. Hulsbergen, Decay chain fitting with a Kalman filter, Nucl. Instrum. Methods Phys. Res., Sect. A **552**, 566 (2005).
[24] L. Breiman, J. H. Friedman, R. A. Olshen, and C. J. Stone, *Classification and Regression Trees* (Wadsworth International Group, Belmont, California, USA, 1984).
[25] A. Hoecker *et al.*, TMVA 4—Toolkit for multivariate data analysis with ROOT. Users guide, arXiv:physics/0703039.
[26] C. Patrignani *et al.* (Particle Data Group Collaboration), Review of particle physics, Chin. Phys. C **40**, 100001 (2016).
[27] W. Verkerke and D. P. Kirkby, The RooFit toolkit for data modeling, eConf **C0303241**, MOLT007 (2003).
[28] T. Skwarnicki, A study of the radiative cascade transitions between the Upsilon-prime and Upsilon resonances, Ph.D thesis, Institute of Nuclear Physics, Krakow, 1986, DESY-F31-86-02.
[29] M. Pivk and F. R. Le Diberder, sPlot: A statistical tool to unfold data distributions, Nucl. Instrum. Methods Phys. Res., Sect. A **555**, 356 (2005).
[30] L. Anderlini *et al.*, The PIDCalib package, Report No. LHCb-PUB-2016-021, 2016.
[31] R. Aaij *et al.*, Selection and processing of calibration samples to measure the particle identification performance of the LHCb experiment in Run 2, Eur. Phys. J. Tech. Instrum. **6**, 1 (2019).
[32] R. Aaij *et al.* (LHCb Collaboration), Observation of a $\Lambda_b^0 - \bar{\Lambda}_b^0$ production asymmetry in proton–proton collisions at $\sqrt{s} = 7$, 8 TeV, Report No. LHCb-PAPER-2021-016, J. High Energy Phys. 10 (2021) 060.
[33] E. Braaten, Y. Jia, and T. Mehen, *B* production asymmetries in perturbative QCD, Phys. Rev. D **66**, 034003 (2002).
[34] W. K. Lai and A. K. Leibovich, Λ_c^+/Λ_c^- and $\Lambda_b^0/\bar{\Lambda}_b^0$ production asymmetry at the LHC from heavy quark recombination, Phys. Rev. D **91**, 054022 (2015).
[35] L. Dufour, High-precision measurements of charge asymmetries at LHCb, Ph.D thesis, Groningen U., 2019.

R. Aaij,[32] A. S. W. Abdelmotteleb,[56] C. Abellán Beteta,[50] F. J. Abudinen Gallego,[56] T. Ackernley,[60] B. Adeva,[46] M. Adinolfi,[54] H. Afsharnia,[9] C. Agapopoulou,[13] C. A. Aidala,[87] S. Aiola,[25] Z. Ajaltouni,[9] S. Akar,[65] J. Albrecht,[15] F. Alessio,[48] M. Alexander,[59] A. Alfonso Albero,[45] Z. Aliouche,[62] G. Alkhazov,[38] P. Alvarez Cartelle,[55] S. Amato,[2] J. L. Amey,[54] Y. Amhis,[11] L. An,[48] L. Anderlini,[22] A. Andreianov,[38] M. Andreotti,[21] F. Archilli,[17] A. Artamonov,[44] M. Artuso,[68] K. Arzymatov,[42] E. Aslanides,[10] M. Atzeni,[50] B. Audurier,[12] S. Bachmann,[17] M. Bachmayer,[49] J. J. Back,[56] P. Baladron Rodriguez,[46] V. Balagura,[12] W. Baldini,[21] J. Baptista Leite,[1] M. Barbetti,[22] R. J. Barlow,[62] S. Barsuk,[11] W. Barter,[61] M. Bartolini,[24,a] F. Baryshnikov,[83] J. M. Basels,[14] S. Bashir,[34] G. Bassi,[29] B. Batsukh,[68] A. Battig,[15] A. Bay,[49] A. Beck,[56] M. Becker,[15] F. Bedeschi,[29] I. Bediaga,[1] A. Beiter,[68] V. Belavin,[42] S. Belin,[27] V. Bellee,[50] K. Belous,[44] I. Belov,[40] I. Belyaev,[41] G. Bencivenni,[23] E. Ben-Haim,[13] A. Berezhnoy,[40] R. Bernet,[50] D. Berninghoff,[17] H. C. Bernstein,[68] C. Bertella,[48] A. Bertolin,[28] C. Betancourt,[50] F. Betti,[48] Ia. Bezshyiko,[50] S. Bhasin,[54] J. Bhom,[35] L. Bian,[73] M. S. Bieker,[15] S. Bifani,[53] P. Billoir,[13] M. Birch,[61] F. C. R. Bishop,[55] A. Bitadze,[62] A. Bizzeti,[22,b] M. Bjørn,[63] M. P. Blago,[48] T. Blake,[56] F. Blanc,[49] S. Blusk,[68] D. Bobulska,[59] J. A. Boelhauve,[15] O. Boente Garcia,[46] T. Boettcher,[65] A. Boldyrev,[82] A. Bondar,[43] N. Bondar,[38,48] S. Borghi,[62] M. Borisyak,[42] M. Borsato,[17] J. T. Borsuk,[35] S. A. Bouchiba,[49] T. J. V. Bowcock,[60] A. Boyer,[48] C. Bozzi,[21] M. J. Bradley,[61] S. Braun,[66] A. Brea Rodriguez,[46] M. Brodski,[48] J. Brodzicka,[35] A. Brossa Gonzalo,[56] D. Brundu,[27] A. Buonaura,[50] L. Buonincontri,[28] A. T. Burke,[62] C. Burr,[48] A. Bursche,[72] A. Butkevich,[39] J. S. Butter,[32] J. Buytaert,[48] W. Byczynski,[48] S. Cadeddu,[27] H. Cai,[73] R. Calabrese,[21,c] L. Calefice,[15,13] L. Calero Diaz,[23] S. Cali,[23] R. Calladine,[53] M. Calvi,[26,d] M. Calvo Gomez,[85] P. Camargo Magalhaes,[54] P. Campana,[23] A. F. Campoverde Quezada,[6] S. Capelli,[26,d] L. Capriotti,[20,e] A. Carbone,[20,e] G. Carboni,[31] R. Cardinale,[24,a] A. Cardini,[27] I. Carli,[4] P. Carniti,[26,d] L. Carus,[14] K. Carvalho Akiba,[32] A. Casais Vidal,[46] G. Casse,[60] M. Cattaneo,[48] G. Cavallero,[48] S. Celani,[49] J. Cerasoli,[10] D. Cervenkov,[63] A. J. Chadwick,[60] M. G. Chapman,[54] M. Charles,[13] Ph. Charpentier,[48] G. Chatzikonstantinidis,[53] C. A. Chavez Barajas,[60] M. Chefdeville,[8] C. Chen,[3] S. Chen,[4] A. Chernov,[35] V. Chobanova,[46] S. Cholak,[49] M. Chrzaszcz,[35] A. Chubykin,[38] V. Chulikov,[38] P. Ciambrone,[23] M. F. Cicala,[56] X. Cid Vidal,[46] G. Ciezarek,[48] P. E. L. Clarke,[58] M. Clemencic,[48] H. V. Cliff,[55] J. Closier,[48] J. L. Cobbledick,[62] V. Coco,[48] J. A. B. Coelho,[11] J. Cogan,[10] E. Cogneras,[9] L. Cojocariu,[37] P. Collins,[48] T. Colombo,[48] L. Congedo,[19,f] A. Contu,[27] N. Cooke,[53] G. Coombs,[59] I. Corredoira,[46] G. Corti,[48] C. M. Costa Sobral,[56] B. Couturier,[48] D. C. Craik,[64] J. Crkovská,[67] M. Cruz Torres,[1] R. Currie,[58] C. L. Da Silva,[67] S. Dadabaev,[83] L. Dai,[71] E. Dall'Occo,[15] J. Dalseno,[46] C. D'Ambrosio,[48] A. Danilina,[41,†] P. d'Argent,[48] J. E. Davies,[62] A. Davis,[62] O. De Aguiar Francisco,[62] K. De Bruyn,[79] S. De Capua,[62] M. De Cian,[49] J. M. De Miranda,[1] L. De Paula,[2] M. De Serio,[19,f] D. De Simone,[50] P. De Simone,[23] J. A. de Vries,[80] C. T. Dean,[67] D. Decamp,[8] V. Dedu,[10] L. Del Buono,[13]

B. Delaney,[55] H.-P. Dembinski,[15] A. Dendek,[34] V. Denysenko,[50] D. Derkach,[82] O. Deschamps,[9] F. Desse,[11] F. Dettori,[27,g] B. Dey,[77] A. Di Cicco,[23] P. Di Nezza,[23] S. Didenko,[83] L. Dieste Maronas,[46] H. Dijkstra,[48] V. Dobishuk,[52] C. Dong,[3] A. M. Donohoe,[18] F. Dordei,[27] A. C. dos Reis,[1] L. Douglas,[59] A. Dovbnya,[51] A. G. Downes,[8] M. W. Dudek,[35] L. Dufour,[48] V. Duk,[78] P. Durante,[48] J. M. Durham,[67] D. Dutta,[62] A. Dziurda,[35] A. Dzyuba,[38] S. Easo,[57] U. Egede,[69] V. Egorychev,[41] S. Eidelman,[43,h] S. Eisenhardt,[58] S. Ek-In,[49] L. Eklund,[59,86] S. Ely,[68] A. Ene,[37] E. Epple,[67] S. Escher,[14] J. Eschle,[50] S. Esen,[13] T. Evans,[48] A. Falabella,[20] J. Fan,[3] Y. Fan,[6] B. Fang,[73] S. Farry,[60] D. Fazzini,[26,d] M. Féo,[48] A. Fernandez Prieto,[46] A. D. Fernez,[66] F. Ferrari,[20,e] L. Ferreira Lopes,[49] F. Ferreira Rodrigues,[2] S. Ferreres Sole,[32] M. Ferrillo,[50] M. Ferro-Luzzi,[48] S. Filippov,[39] R. A. Fini,[19] M. Fiorini,[21,c] M. Firlej,[34] K. M. Fischer,[63] D. S. Fitzgerald,[87] C. Fitzpatrick,[62] T. Fiutowski,[34] A. Fkiaras,[48] F. Fleuret,[12] M. Fontana,[13] F. Fontanelli,[24,a] R. Forty,[48] D. Foulds-Holt,[55] V. Franco Lima,[60] M. Franco Sevilla,[66] M. Frank,[48] E. Franzoso,[21] G. Frau,[17] C. Frei,[48] D. A. Friday,[59] J. Fu,[6] Q. Fuehring,[15] E. Gabriel,[32] A. Gallas Torreira,[46] D. Galli,[20,e] S. Gambetta,[58,48] Y. Gan,[3] M. Gandelman,[2] P. Gandini,[25] Y. Gao,[5] M. Garau,[27] L. M. Garcia Martin,[56] P. Garcia Moreno,[45] J. García Pardiñas,[26,d] B. Garcia Plana,[46] F. A. Garcia Rosales,[12] L. Garrido,[45] C. Gaspar,[48] R. E. Geertsema,[32] D. Gerick,[17] L. L. Gerken,[15] E. Gersabeck,[62] M. Gersabeck,[62] T. Gershon,[56] D. Gerstel,[10] Ph. Ghez,[8] L. Giambastiani,[28] V. Gibson,[55] H. K. Giemza,[36] A. L. Gilman,[63] M. Giovannetti,[23,i] A. Gioventù,[46] P. Gironella Gironell,[45] L. Giubega,[37] C. Giugliano,[21,48,c] K. Gizdov,[58] E. L. Gkougkousis,[48] V. V. Gligorov,[13] C. Göbel,[70] E. Golobardes,[85] D. Golubkov,[41] A. Golutvin,[61,83] A. Gomes,[1,j] S. Gomez Fernandez,[45] F. Goncalves Abrantes,[63] M. Goncerz,[35] G. Gong,[3] P. Gorbounov,[41] I. V. Gorelov,[40] C. Gotti,[26] E. Govorkova,[48] J. P. Grabowski,[17] T. Grammatico,[13] L. A. Granado Cardoso,[48] E. Graugés,[45] E. Graverini,[49] G. Graziani,[22] A. Grecu,[37] L. M. Greeven,[32] N. A. Grieser,[4] L. Grillo,[62] S. Gromov,[83] B. R. Gruberg Cazon,[63] C. Gu,[3] M. Guarise,[21] M. Guittiere,[11] P. A. Günther,[17] E. Gushchin,[39] A. Guth,[14] Y. Guz,[44] T. Gys,[48] T. Hadavizadeh,[69] G. Haefeli,[49] C. Haen,[48] J. Haimberger,[48] T. Halewood-leagas,[60] P. M. Hamilton,[66] J. P. Hammerich,[60] Q. Han,[7] X. Han,[17] T. H. Hancock,[63] S. Hansmann-Menzemer,[17] N. Harnew,[63] T. Harrison,[60] C. Hasse,[48] M. Hatch,[48] J. He,[6,k] M. Hecker,[61] K. Heijhoff,[32] K. Heinicke,[15] A. M. Hennequin,[48] K. Hennessy,[60] L. Henry,[48] J. Heuel,[14] A. Hicheur,[2] D. Hill,[49] M. Hilton,[62] S. E. Hollitt,[15] R. Hou,[7] Y. Hou,[6] J. Hu,[17] J. Hu,[72] W. Hu,[7] X. Hu,[3] W. Huang,[6] X. Huang,[73] W. Hulsbergen,[32] R. J. Hunter,[56] M. Hushchyn,[82] D. Hutchcroft,[60] D. Hynds,[32] P. Ibis,[15] M. Idzik,[34] D. Ilin,[38] P. Ilten,[65] A. Inglessi,[38] A. Ishteev,[83] K. Ivshin,[38] R. Jacobsson,[48] H. Jage,[14] S. Jakobsen,[48] E. Jans,[32] B. K. Jashal,[47] A. Jawahery,[66] V. Jevtic,[15] F. Jiang,[3] M. John,[63] D. Johnson,[48] C. R. Jones,[55] T. P. Jones,[56] B. Jost,[48] N. Jurik,[48] S. H. Kalavan Kadavath,[34] S. Kandybei,[51] Y. Kang,[3] M. Karacson,[48] M. Karpov,[82] F. Keizer,[48] D. M. Keller,[68] M. Kenzie,[56] T. Ketel,[33] B. Khanji,[15] A. Kharisova,[84] S. Kholodenko,[44] T. Kirn,[14] V. S. Kirsebom,[49] O. Kitouni,[64] S. Klaver,[32] N. Kleijne,[29] K. Klimaszewski,[36] M. R. Kmiec,[36] S. Koliiev,[52] A. Kondybayeva,[83] A. Konoplyannikov,[41] P. Kopciewicz,[34] R. Kopecna,[17] P. Koppenburg,[32] M. Korolev,[40] I. Kostiuk,[32,52] O. Kot,[52] S. Kotriakhova,[21,38] P. Kravchenko,[38] L. Kravchuk,[39] R. D. Krawczyk,[48] M. Kreps,[56] F. Kress,[61] S. Kretzschmar,[14] P. Krokovny,[43,h] W. Krupa,[34] W. Krzemien,[36] M. Kucharczyk,[35] V. Kudryavtsev,[43,h] H. S. Kuindersma,[32,33] G. J. Kunde,[67] T. Kvaratskheliya,[41] D. Lacarrere,[48] G. Lafferty,[62] A. Lai,[27] A. Lampis,[27] D. Lancierini,[50] J. J. Lane,[62] R. Lane,[54] G. Lanfranchi,[23] C. Langenbruch,[14] J. Langer,[15] O. Lantwin,[83] T. Latham,[56] F. Lazzari,[29,l] R. Le Gac,[10] S. H. Lee,[87] R. Lefèvre,[9] A. Leflat,[40] S. Legotin,[83] O. Leroy,[10] T. Lesiak,[35] B. Leverington,[17] H. Li,[72] P. Li,[17] S. Li,[7] Y. Li,[4] Y. Li,[4] Z. Li,[68] X. Liang,[68] T. Lin,[61] R. Lindner,[48] V. Lisovskyi,[15] R. Litvinov,[27] G. Liu,[72] H. Liu,[6] Q. Liu,[6] S. Liu,[4] A. Lobo Salvia,[45] A. Loi,[27] J. Lomba Castro,[46] I. Longstaff,[59] J. H. Lopes,[2] S. Lopez Solino,[46] G. H. Lovell,[55] Y. Lu,[4] C. Lucarelli,[22] D. Lucchesi,[28,m] S. Luchuk,[39] M. Lucio Martinez,[32] V. Lukashenko,[32,52] Y. Luo,[3] A. Lupato,[62] E. Luppi,[21,c] O. Lupton,[56] A. Lusiani,[29,n] X. Lyu,[6] L. Ma,[4] R. Ma,[6] S. Maccolini,[20,e] F. Machefert,[11] F. Maciuc,[37] V. Macko,[49] P. Mackowiak,[15] S. Maddrell-Mander,[54] O. Madejczyk,[34] L. R. Madhan Mohan,[54] O. Maev,[38] A. Maevskiy,[82] D. Maisuzenko,[38] M. W. Majewski,[34] J. J. Malczewski,[35] S. Malde,[63] B. Malecki,[48] A. Malinin,[81] T. Maltsev,[43,h] H. Malygina,[17] G. Manca,[27,g] G. Mancinelli,[10] D. Manuzzi,[20,e] D. Marangotto,[25,o] J. Maratas,[9,p] J. F. Marchand,[8] U. Marconi,[20] S. Mariani,[22,q] C. Marin Benito,[48] M. Marinangeli,[49] J. Marks,[17] A. M. Marshall,[54] P. J. Marshall,[60] G. Martelli,[78] G. Martellotti,[30] L. Martinazzoli,[48,d] M. Martinelli,[26,d] D. Martinez Santos,[46] F. Martinez Vidal,[47] A. Massafferri,[1] M. Materok,[14] R. Matev,[48] A. Mathad,[50] Z. Mathe,[48] V. Matiunin,[41] C. Matteuzzi,[26] K. R. Mattioli,[87] A. Mauri,[32] E. Maurice,[12] J. Mauricio,[45] M. Mazurek,[48] M. McCann,[61] L. Mcconnell,[18] T. H. Mcgrath,[62] N. T. Mchugh,[59] A. McNab,[62] R. McNulty,[18] J. V. Mead,[60] B. Meadows,[65] G. Meier,[15] N. Meinert,[76] D. Melnychuk,[36] S. Meloni,[26,d] M. Merk,[32,80] A. Merli,[25,o] L. Meyer Garcia,[2] M. Mikhasenko,[48] D. A. Milanes,[74] E. Millard,[56] M. Milovanovic,[48] M.-N. Minard,[8] A. Minotti,[26,d] L. Minzoni,[21,c] S. E. Mitchell,[58] B. Mitreska,[62] D. S. Mitzel,[48] A. Mödden,[15] R. A. Mohammed,[63] R. D. Moise,[61] S. Mokhnenko,[82] T. Mombächer,[46]

I. A. Monroy,[74] S. Monteil,[9] M. Morandin,[28] G. Morello,[23] M. J. Morello,[29,n] J. Moron,[34] A. B. Morris,[75] A. G. Morris,[56] R. Mountain,[68] H. Mu,[3] F. Muheim,[58,48] M. Mulder,[48] D. Müller,[48] K. Müller,[50] C. H. Murphy,[63] D. Murray,[62] P. Muzzetto,[27,48] P. Naik,[54] T. Nakada,[49] R. Nandakumar,[57] T. Nanut,[49] I. Nasteva,[2] M. Needham,[58] I. Neri,[21] N. Neri,[25,o] S. Neubert,[75] N. Neufeld,[48] R. Newcombe,[61] T. D. Nguyen,[49] C. Nguyen-Mau,[49,r] E. M. Niel,[11] S. Nieswand,[14] N. Nikitin,[40] N. S. Nolte,[64] C. Normand,[8] C. Nunez,[87] A. Oblakowska-Mucha,[34] V. Obraztsov,[44] T. Oeser,[14] D. P. O'Hanlon,[54] S. Okamura,[21] R. Oldeman,[27,g] F. Oliva,[58] M. E. Olivares,[68] C. J. G. Onderwater,[79] R. H. O'Neil,[58] J. M. Otalora Goicochea,[2] T. Ovsiannikova,[41] P. Owen,[50] A. Oyanguren,[47] K. O. Padeken,[75] B. Pagare,[56] P. R. Pais,[48] T. Pajero,[63] A. Palano,[19] M. Palutan,[23] Y. Pan,[62] G. Panshin,[84] A. Papanestis,[57] M. Pappagallo,[19,f] L. L. Pappalardo,[21,c] C. Pappenheimer,[65] W. Parker,[66] C. Parkes,[62] B. Passalacqua,[21] G. Passaleva,[22] A. Pastore,[19] M. Patel,[61] C. Patrignani,[20,e] C. J. Pawley,[80] A. Pearce,[48] A. Pellegrino,[32] M. Pepe Altarelli,[48] S. Perazzini,[20] D. Pereima,[41] A. Pereiro Castro,[46] P. Perret,[9] M. Petric,[59,48] K. Petridis,[54] A. Petrolini,[24,a] A. Petrov,[81] S. Petrucci,[58] M. Petruzzo,[25] T. T. H. Pham,[68] A. Philippov,[42] L. Pica,[29,n] M. Piccini,[78] B. Pietrzyk,[8] G. Pietrzyk,[49] M. Pili,[63] D. Pinci,[30] F. Pisani,[48] M. Pizzichemi,[26,48,d] Resmi P. K,[10] V. Placinta,[37] J. Plews,[53] M. Plo Casasus,[46] F. Polci,[13] M. Poli Lener,[23] M. Poliakova,[68] A. Poluektov,[10] N. Polukhina,[83,s] I. Polyakov,[68] E. Polycarpo,[2] S. Ponce,[48] D. Popov,[6,48] S. Popov,[42] S. Poslavskii,[44] K. Prasanth,[35] L. Promberger,[48] C. Prouve,[46] V. Pugatch,[52] V. Puill,[11] H. Pullen,[63] G. Punzi,[29,t] H. Qi,[3] W. Qian,[6] J. Qin,[6] N. Qin,[3] R. Quagliani,[49] B. Quintana,[8] N. V. Raab,[18] R. I. Rabadan Trejo,[6] B. Rachwal,[34] J. H. Rademacker,[54] M. Rama,[29] M. Ramos Pernas,[56] M. S. Rangel,[2] F. Ratnikov,[42,82] G. Raven,[33] M. Reboud,[8] F. Redi,[49] F. Reiss,[62] C. Remon Alepuz,[47] Z. Ren,[3] V. Renaudin,[63] R. Ribatti,[29] S. Ricciardi,[57] K. Rinnert,[60] P. Robbe,[11] G. Robertson,[58] A. B. Rodrigues,[49] E. Rodrigues,[60] J. A. Rodriguez Lopez,[74] E. R. R. Rodriguez Rodriguez,[46] M. Roehrken,[48] A. Rollings,[63] P. Roloff,[48] V. Romanovskiy,[44] M. Romero Lamas,[46] A. Romero Vidal,[46] J. D. Roth,[87] M. Rotondo,[23] M. S. Rudolph,[68] T. Ruf,[48] R. A. Ruiz Fernandez,[46] J. Ruiz Vidal,[47] A. Ryzhikov,[82] J. Ryzka,[34] J. J. Saborido Silva,[46] N. Sagidova,[38] N. Sahoo,[56] B. Saitta,[27,g] M. Salomoni,[48] C. Sanchez Gras,[32] R. Santacesaria,[30] C. Santamarina Rios,[46] M. Santimaria,[23] E. Santovetti,[31,i] D. Saranin,[83] G. Sarpis,[14] M. Sarpis,[75] A. Sarti,[30] C. Satriano,[30,u] A. Satta,[31] M. Saur,[15] D. Savrina,[41,40] H. Sazak,[9] L. G. Scantlebury Smead,[63] A. Scarabotto,[13] S. Schael,[14] S. Scherl,[60] M. Schiller,[59] H. Schindler,[48] M. Schmelling,[16] B. Schmidt,[48] S. Schmitt,[14] O. Schneider,[49] A. Schopper,[48] M. Schubiger,[32] S. Schulte,[49] M. H. Schune,[11] R. Schwemmer,[48] B. Sciascia,[23,48] S. Sellam,[46] A. Semennikov,[41] M. Senghi Soares,[33] A. Sergi,[24,a] N. Serra,[50] L. Sestini,[28] A. Seuthe,[15] Y. Shang,[5] D. M. Shangase,[87] M. Shapkin,[44] I. Shchemerov,[83] L. Shchutska,[49] T. Shears,[60] L. Shekhtman,[43,h] Z. Shen,[5] V. Shevchenko,[81] E. B. Shields,[26,d] Y. Shimizu,[11] E. Shmanin,[83] J. D. Shupperd,[68] B. G. Siddi,[21] R. Silva Coutinho,[50] G. Simi,[28] S. Simone,[19,f] E Sirks,[48] N. Skidmore,[62] T. Skwarnicki,[68] M. W. Slater,[53] I. Slazyk,[21,c] J. C. Smallwood,[63] J. G. Smeaton,[55] A. Smetkina,[41] E. Smith,[50] M. Smith,[61] A. Snoch,[32] M. Soares,[20] L. Soares Lavra,[9] M. D. Sokoloff,[65] F. J. P. Soler,[59] A. Solovev,[38] I. Solovyev,[38] F. L. Souza De Almeida,[2] B. Souza De Paula,[2] B. Spaan,[15] E. Spadaro Norella,[25,o] P. Spradlin,[59] F. Stagni,[48] M. Stahl,[65] S. Stahl,[48] S. Stanislaus,[63] O. Steinkamp,[50,83] O. Stenyakin,[44] H. Stevens,[15] S. Stone,[68] M. Straticiuc,[37] D. Strekalina,[83] F. Suljik,[63] J. Sun,[27] L. Sun,[73] Y. Sun,[66] P. Svihra,[62] P. N. Swallow,[53] K. Swientek,[34] A. Szabelski,[36] T. Szumlak,[34] M. Szymanski,[48] S. Taneja,[62] A. R. Tanner,[54] M. D. Tat,[63] A. Terentev,[83] F. Teubert,[48] E. Thomas,[48] D. J. D. Thompson,[53] K. A. Thomson,[60] V. Tisserand,[9] S. T'Jampens,[8] M. Tobin,[4] L. Tomassetti,[21,c] X. Tong,[5] D. Torres Machado,[1] D. Y. Tou,[13] M. T. Tran,[49] E. Trifonova,[83] C. Trippl,[49] G. Tuci,[6] A. Tully,[49] N. Tuning,[32,48] A. Ukleja,[36] D. J. Unverzagt,[17] E. Ursov,[83] A. Usachov,[32] A. Ustyuzhanin,[42,82] U. Uwer,[17] A. Vagner,[84] V. Vagnoni,[20] A. Valassi,[48] G. Valenti,[20] N. Valls Canudas,[85] M. van Beuzekom,[32] M. Van Dijk,[49] E. van Herwijnen,[83] C. B. Van Hulse,[18] M. van Veghel,[79] R. Vazquez Gomez,[45] P. Vazquez Regueiro,[46] C. Vázquez Sierra,[48] S. Vecchi,[21] J. J. Velthuis,[54] M. Veltri,[22,v] A. Venkateswaran,[68] M. Veronesi,[32] M. Vesterinen,[56] D. Vieira,[65] M. Vieites Diaz,[49] H. Viemann,[76] X. Vilasis-Cardona,[85] E. Vilella Figueras,[60] A. Villa,[20] P. Vincent,[13] F. C. Volle,[11] D. Vom Bruch,[10] A. Vorobyev,[38] V. Vorobyev,[43,h] N. Voropaev,[38] K. Vos,[80] R. Waldi,[17] J. Walsh,[29] C. Wang,[17] J. Wang,[5] J. Wang,[4] J. Wang,[3] J. Wang,[73] M. Wang,[3] R. Wang,[54] Y. Wang,[7] Z. Wang,[50] Z. Wang,[3] Z. Wang,[6] J. A. Ward,[56] N. K. Watson,[53] S. G. Weber,[13] D. Websdale,[61] C. Weisser,[64] B. D. C. Westhenry,[54] D. J. White,[62] M. Whitehead,[54] A. R. Wiederhold,[56] D. Wiedner,[15] G. Wilkinson,[63] M. Wilkinson,[68] I. Williams,[55] M. Williams,[64] M. R. J. Williams,[58] F. F. Wilson,[57] W. Wislicki,[36] M. Witek,[35] L. Witola,[17] G. Wormser,[11] S. A. Wotton,[55] H. Wu,[68] K. Wyllie,[48] Z. Xiang,[6] D. Xiao,[7] Y. Xie,[7] A. Xu,[5] J. Xu,[6] L. Xu,[3] M. Xu,[7] Q. Xu,[6] Z. Xu,[5] Z. Xu,[6] D. Yang,[3] S. Yang,[6] Y. Yang,[6] Z. Yang,[5] Z. Yang,[66] Y. Yao,[68] L. E. Yeomans,[60] H. Yin,[7] J. Yu,[71] X. Yuan,[68] O. Yushchenko,[44] E. Zaffaroni,[49] M. Zavertyaev,[16,s] M. Zdybal,[35] O. Zenaiev,[48] M. Zeng,[3] D. Zhang,[7] L. Zhang,[3] S. Zhang,[71] S. Zhang,[5] Y. Zhang,[5] Y. Zhang,[63] A. Zharkova,[83] A. Zhelezov,[17] Y. Zheng,[6] T. Zhou,[5]

X. Zhou,[6] Y. Zhou,[6] V. Zhovkovska,[11] X. Zhu,[3] X. Zhu,[7] Z. Zhu,[6] V. Zhukov,[14,40] J. B. Zonneveld,[58] Q. Zou,[4] S. Zucchelli,[20,e] D. Zuliani,[28] and G. Zunica[62]

(LHCb Collaboration)

[1]*Centro Brasileiro de Pesquisas Físicas (CBPF), Rio de Janeiro, Brazil*
[2]*Universidade Federal do Rio de Janeiro (UFRJ), Rio de Janeiro, Brazil*
[3]*Center for High Energy Physics, Tsinghua University, Beijing, China*
[4]*Institute Of High Energy Physics (IHEP), Beijing, China*
[5]*School of Physics State Key Laboratory of Nuclear Physics and Technology, Peking University, Beijing, China*
[6]*University of Chinese Academy of Sciences, Beijing, China*
[7]*Institute of Particle Physics, Central China Normal University, Wuhan, Hubei, China*
[8]*Univ. Savoie Mont Blanc, CNRS, IN2P3-LAPP, Annecy, France*
[9]*Université Clermont Auvergne, CNRS/IN2P3, LPC, Clermont-Ferrand, France*
[10]*Aix Marseille Univ, CNRS/IN2P3, CPPM, Marseille, France*
[11]*Université Paris-Saclay, CNRS/IN2P3, IJCLab, Orsay, France*
[12]*Laboratoire Leprince-Ringuet, CNRS/IN2P3, Ecole Polytechnique, Institut Polytechnique de Paris, Palaiseau, France*
[13]*LPNHE, Sorbonne Université, Paris Diderot Sorbonne Paris Cité, CNRS/IN2P3, Paris, France*
[14]*I. Physikalisches Institut, RWTH Aachen University, Aachen, Germany*
[15]*Fakultät Physik, Technische Universität Dortmund, Dortmund, Germany*
[16]*Max-Planck-Institut für Kernphysik (MPIK), Heidelberg, Germany*
[17]*Physikalisches Institut, Ruprecht-Karls-Universität Heidelberg, Heidelberg, Germany*
[18]*School of Physics, University College Dublin, Dublin, Ireland*
[19]*INFN Sezione di Bari, Bari, Italy*
[20]*INFN Sezione di Bologna, Bologna, Italy*
[21]*INFN Sezione di Ferrara, Ferrara, Italy*
[22]*INFN Sezione di Firenze, Firenze, Italy*
[23]*INFN Laboratori Nazionali di Frascati, Frascati, Italy*
[24]*INFN Sezione di Genova, Genova, Italy*
[25]*INFN Sezione di Milano, Milano, Italy*
[26]*INFN Sezione di Milano-Bicocca, Milano, Italy*
[27]*INFN Sezione di Cagliari, Monserrato, Italy*
[28]*Universita degli Studi di Padova, Universita e INFN, Padova, Padova, Italy*
[29]*INFN Sezione di Pisa, Pisa, Italy*
[30]*INFN Sezione di Roma La Sapienza, Roma, Italy*
[31]*INFN Sezione di Roma Tor Vergata, Roma, Italy*
[32]*Nikhef National Institute for Subatomic Physics, Amsterdam, Netherlands*
[33]*Nikhef National Institute for Subatomic Physics and VU University Amsterdam, Amsterdam, Netherlands*
[34]*AGH—University of Science and Technology, Faculty of Physics and Applied Computer Science, Kraków, Poland*
[35]*Henryk Niewodniczanski Institute of Nuclear Physics Polish Academy of Sciences, Kraków, Poland*
[36]*National Center for Nuclear Research (NCBJ), Warsaw, Poland*
[37]*Horia Hulubei National Institute of Physics and Nuclear Engineering, Bucharest-Magurele, Romania*
[38]*Petersburg Nuclear Physics Institute NRC Kurchatov Institute (PNPI NRC KI), Gatchina, Russia*
[39]*Institute for Nuclear Research of the Russian Academy of Sciences (INR RAS), Moscow, Russia*
[40]*Institute of Nuclear Physics, Moscow State University (SINP MSU), Moscow, Russia*
[41]*Institute of Theoretical and Experimental Physics NRC Kurchatov Institute (ITEP NRC KI), Moscow, Russia*
[42]*Yandex School of Data Analysis, Moscow, Russia*
[43]*Budker Institute of Nuclear Physics (SB RAS), Novosibirsk, Russia*
[44]*Institute for High Energy Physics NRC Kurchatov Institute (IHEP NRC KI), Protvino, Russia, Protvino, Russia*
[45]*ICCUB, Universitat de Barcelona, Barcelona, Spain*
[46]*Instituto Galego de Física de Altas Enerxías (IGFAE), Universidade de Santiago de Compostela, Santiago de Compostela, Spain*
[47]*Instituto de Fisica Corpuscular, Centro Mixto Universidad de Valencia—CSIC, Valencia, Spain*
[48]*European Organization for Nuclear Research (CERN), Geneva, Switzerland*

[49]Institute of Physics, Ecole Polytechnique Fédérale de Lausanne (EPFL), Lausanne, Switzerland
[50]Physik-Institut, Universität Zürich, Zürich, Switzerland
[51]NSC Kharkiv Institute of Physics and Technology (NSC KIPT), Kharkiv, Ukraine
[52]Institute for Nuclear Research of the National Academy of Sciences (KINR), Kyiv, Ukraine
[53]University of Birmingham, Birmingham, United Kingdom
[54]H.H. Wills Physics Laboratory, University of Bristol, Bristol, United Kingdom
[55]Cavendish Laboratory, University of Cambridge, Cambridge, United Kingdom
[56]Department of Physics, University of Warwick, Coventry, United Kingdom
[57]STFC Rutherford Appleton Laboratory, Didcot, United Kingdom
[58]School of Physics and Astronomy, University of Edinburgh, Edinburgh, United Kingdom
[59]School of Physics and Astronomy, University of Glasgow, Glasgow, United Kingdom
[60]Oliver Lodge Laboratory, University of Liverpool, Liverpool, United Kingdom
[61]Imperial College London, London, United Kingdom
[62]Department of Physics and Astronomy, University of Manchester, Manchester, United Kingdom
[63]Department of Physics, University of Oxford, Oxford, United Kingdom
[64]Massachusetts Institute of Technology, Cambridge, Massachusetts, USA
[65]University of Cincinnati, Cincinnati, Ohio, USA
[66]University of Maryland, College Park, Maryland, USA
[67]Los Alamos National Laboratory (LANL), Los Alamos, New Mexico, USA
[68]Syracuse University, Syracuse, New York, USA
[69]School of Physics and Astronomy, Monash University, Melbourne, Australia
(associated with Institution Department of Physics, University of Warwick, Coventry, United Kingdom)
[70]Pontifícia Universidade Católica do Rio de Janeiro (PUC-Rio), Rio de Janeiro, Brazil
[associated with Universidade Federal do Rio de Janeiro (UFRJ), Rio de Janeiro, Brazil]
[71]Physics and Micro Electronic College, Hunan University, Changsha City, China (associated with Institute of Particle Physics, Central China Normal University, Wuhan, Hubei, China)
[72]Guangdong Provincial Key Laboratory of Nuclear Science, Guangdong-Hong Kong Joint Laboratory of Quantum Matter, Institute of Quantum Matter, South China Normal University, Guangzhou, China (associated with Center for High Energy Physics, Tsinghua University, Beijing, China)
[73]School of Physics and Technology, Wuhan University, Wuhan, China (associated with Center for High Energy Physics, Tsinghua University, Beijing, China)
[74]Departamento de Fisica, Universidad Nacional de Colombia, Bogota, Colombia (associated with LPNHE, Sorbonne Université, Paris Diderot Sorbonne Paris Cité, CNRS/IN2P3, Paris, France)
[75]Universität Bonn—Helmholtz-Institut für Strahlen und Kernphysik, Bonn, Germany (associated with Physikalisches Institut, Ruprecht-Karls-Universität Heidelberg, Heidelberg, Germany)
[76]Institut für Physik, Universität Rostock, Rostock, Germany (associated with Physikalisches Institut, Ruprecht-Karls-Universität Heidelberg, Heidelberg, Germany)
[77]Eotvos Lorand University, Budapest, Hungary [associated with European Organization for Nuclear Research (CERN), Geneva, Switzerland]
[78]INFN Sezione di Perugia, Perugia, Italy (associated with INFN Sezione di Ferrara, Ferrara, Italy)
[79]Van Swinderen Institute, University of Groningen, Groningen, Netherlands (associated with Nikhef National Institute for Subatomic Physics, Amsterdam, Netherlands)
[80]Universiteit Maastricht, Maastricht, Netherlands (associated with Nikhef National Institute for Subatomic Physics, Amsterdam, Netherlands)
[81]National Research Centre Kurchatov Institute, Moscow, Russia [associated with Institute of Theoretical and Experimental Physics NRC Kurchatov Institute (ITEP NRC KI), Moscow, Russia]
[82]National Research University Higher School of Economics, Moscow, Russia (associated with Yandex School of Data Analysis, Moscow, Russia)
[83]National University of Science and Technology "MISIS", Moscow, Russia [associated with Institute of Theoretical and Experimental Physics NRC Kurchatov Institute (ITEP NRC KI), Moscow, Russia]
[84]National Research Tomsk Polytechnic University, Tomsk, Russia [associated with Institute of Theoretical and Experimental Physics NRC Kurchatov Institute (ITEP NRC KI), Moscow, Russia]
[85]DS4DS, La Salle, Universitat Ramon Llull, Barcelona, Spain
(associated with ICCUB, Universitat de Barcelona, Barcelona, Spain)
[86]Department of Physics and Astronomy, Uppsala University, Uppsala, Sweden (associated with School of Physics and Astronomy, University of Glasgow, Glasgow, United Kingdom)
[87]University of Michigan, Ann Arbor, Michigan, USA (associated with Syracuse University, Syracuse, New York, USA)

[a]Also at Università di Genova, Genova, Italy.
[b]Also at Università di Modena e Reggio Emilia, Modena, Italy.
[c]Also at Università di Ferrara, Ferrara, Italy.
[d]Also at Università di Milano Bicocca, Milano, Italy.
[e]Also at Università di Bologna, Bologna, Italy.
[f]Also at Università di Bari, Bari, Italy.
[g]Also at Università di Cagliari, Cagliari, Italy.
[h]Also at Novosibirsk State University, Novosibirsk, Russia.
[i]Also at Università di Roma Tor Vergata, Roma, Italy.
[j]Also at Universidade Federal do Triângulo Mineiro (UFTM), Uberaba-MG, Brazil.
[k]Also at Hangzhou Institute for Advanced Study, UCAS, Hangzhou, China.
[l]Also at Università di Siena, Siena, Italy.
[m]Also at Università di Padova, Padova, Italy.
[n]Also at Scuola Normale Superiore, Pisa, Italy.
[o]Also at Università degli Studi di Milano, Milano, Italy.
[p]Also at MSU—Iligan Institute of Technology (MSU-IIT), Iligan, Philippines.
[q]Also at Università di Firenze, Firenze, Italy.
[r]Also at Hanoi University of Science, Hanoi, Vietnam.
[s]Also at P.N. Lebedev Physical Institute, Russian Academy of Science (LPI RAS), Moscow, Russia.
[t]Also at Università di Pisa, Pisa, Italy.
[u]Also at Università della Basilicata, Potenza, Italy.
[v]Also at Università di Urbino, Urbino, Italy.
[†]Corresponding author.
daniel.johnson@cern.ch